Supporting Information

A Sillén Oxyhalide $SrBi_3O_4Cl_3$ as a Promising Photocatalyst for Water Splitting: Impact of the Asymmetric Structure on Light Absorption and Charge Carrier Dynamics

Hajime Suzuki,[a] Daichi Ozaki,[a] Yusuke Ishii,[a] Osamu Tomita,[a] Daichi Kato,[a] Shunsuke Nozawa,[b] Kouichi Nakashima,[c] Akinori Saeki,[d] Hiroshi Kageyama,[a] Ryu Abe[a,*]

a. Department of Energy and Hydrocarbon Chemistry, Graduate School of Engineering, Kyoto University, Nishikyo-ku, Kyoto 615-8510, Japan
b. Photon Factory (PF), Institute of Materials Structure Science (IMSS), High Energy Accelerator Research Organization (KEK), Tsukuba, Ibaraki 305-0801, Japan
c. Department of Materials Science and Engineering, Graduate School of Science and Engineering, Ibaraki University, 4-12-1, Nakanarusawa, Hitachi, Ibaraki 316-8511, Japan
d. Department of Applied Chemistry, Graduate School of Engineering, Osaka University, 2-1 Yamadaoka, Suita, Osaka 565-0871, Japan

† H. S. and D. O. contributed equally to this work.

Table S1 Final refined structure parameters for $SrBi_3O_4Cl_3$[a]

Atom	Site	*x*	*y*	*z*	*g*	100*U* / Å²
Bi/Sr2	4*e*	0	0	Bi: 0.3432(10) Sr: 0.3287(3)	Bi: 0.528(2) Sr: 0.472 (2)	1.54(6)
Bi/Sr1	4*e*	0	0	Bi: 0.07170(8) Sr: 0.080(6)	Bi: 0.972(2) Sr: 0.028(2)	1.76(4)
Cl2	4*e*	0	0	0.2100(3)	1	1.1(13)
Cl1	2*b*	0	0	1/2	1	1.1(13)
O1	8*g*	0	1/2	0.1114(5)	1	1.1(13)

[a]Space group *I*4/*mmm* (#139), tetragonal, $a = b = 3.93319(4)$ Å, $c = 27.0186(6)$ Å, $V = 417.98(11)$ Å³.

Table S2 Bond valence sum of Bi and Sr in Bi/Sr1 and Bi/Sr2 sites.

Atom	Bond valence sum
Bi in Bi/Sr1	3.03
Bi in Bi/Sr2	2.88
Sr in Bi/Sr1	3.93
Sr in Bi/Sr2	2.41

Table S3 Rate constants and lifetimes obtained from the fitting of the TRMC kinetics (Figure S16). The effective lifetime (τ_{eff}) was calculated using $\tau_{eff} = (A_1 + A_2)(A_1k_1 + A_2k_2)^{-1}$. The maximum signal intensity of TRMC transients (Figure 8) ($\varphi\Sigma\mu_{max}$) and the product of $\varphi\Sigma\mu_{max}$ and τ_{eff} ($\varphi\Sigma\mu_{max}\times\tau_{eff}$) are also listed.

	$SrBi_3O_4Cl_3$	BiOCl	$SrBiO_2Cl$
k_1 (s^{-1})	2.3×10^{6}	1.7×10^{7}	1.9×10^{6}
k_2 (s^{-1})	4.7×10^{4}	1.1×10^{5}	4.0×10^{4}
τ_{eff} (s)	1.1×10^{-5}	6.0×10^{-7}	1.1×10^{-5}
$\varphi\Sigma\mu_{max}$ ($m^2V^{-1}s^{-1}$)	4.1×10^{-7}	2.7×10^{-7}	1.9×10^{-8}
$\varphi\Sigma\mu_{max}\times\tau_{eff}$ (m^2V^{-1})	4.5×10^{-12}	1.6×10^{-13}	2.1×10^{-13}

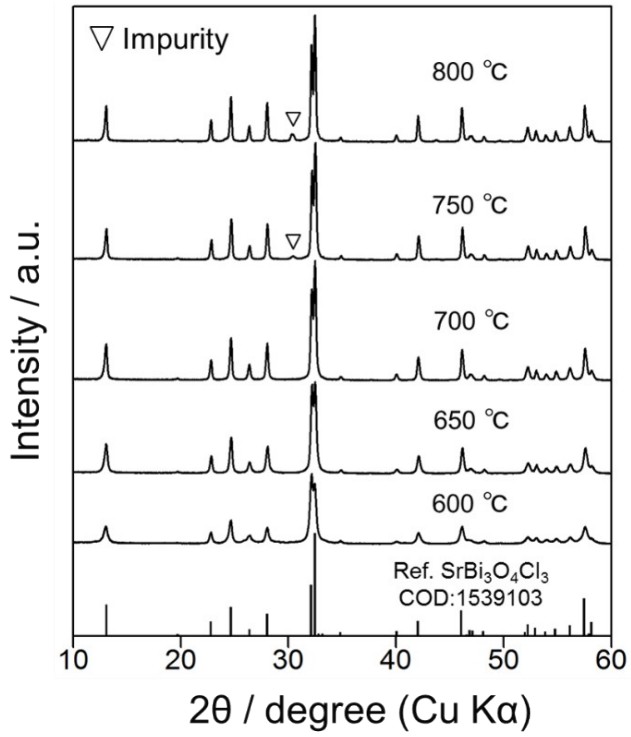

Figure S1 XRD patterns of $SrBi_3O_4Cl_3$ samples prepared at 600−800 °C. The $SrBi_3O_4Cl_3$ sample prepared at 700 °C was used in the present study.

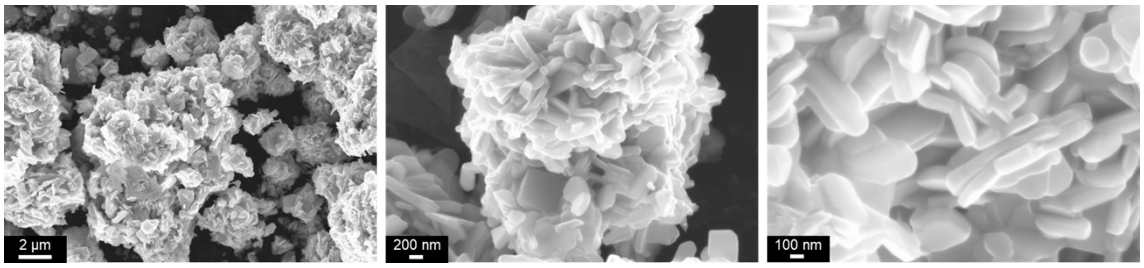

Figure S2 SEM images of the $SrBi_3O_4Cl_3$ sample prepared at 700 °C.

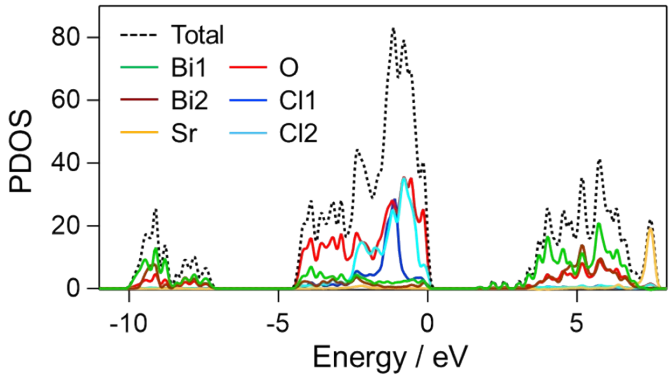

Figure S3 DOS and PDOS of $SrBi_3O_4Cl_3$ calculated using the Quantum Espresso package.

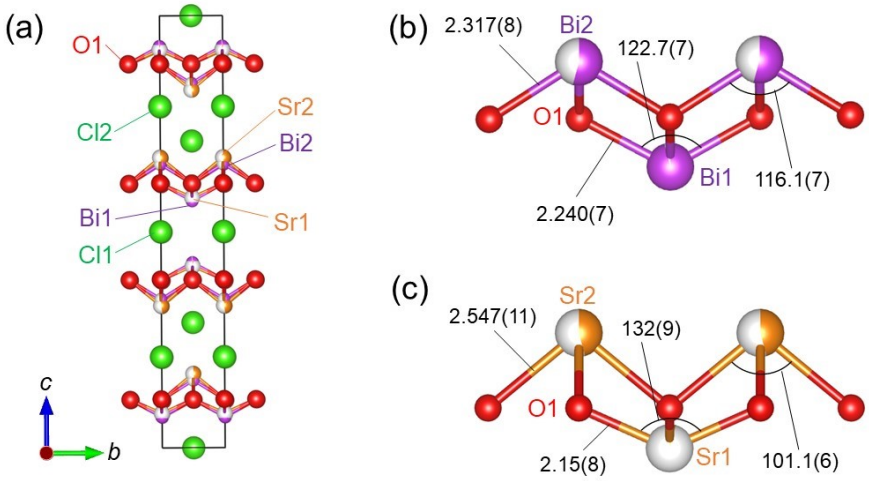

Figure S4 (a) Refined crystal structure of $SrBi_3O_4Cl_3$, and coordination environments around (b) Bi1 and Bi2, and (c) Sr1 and Sr2 (in Å and degree).

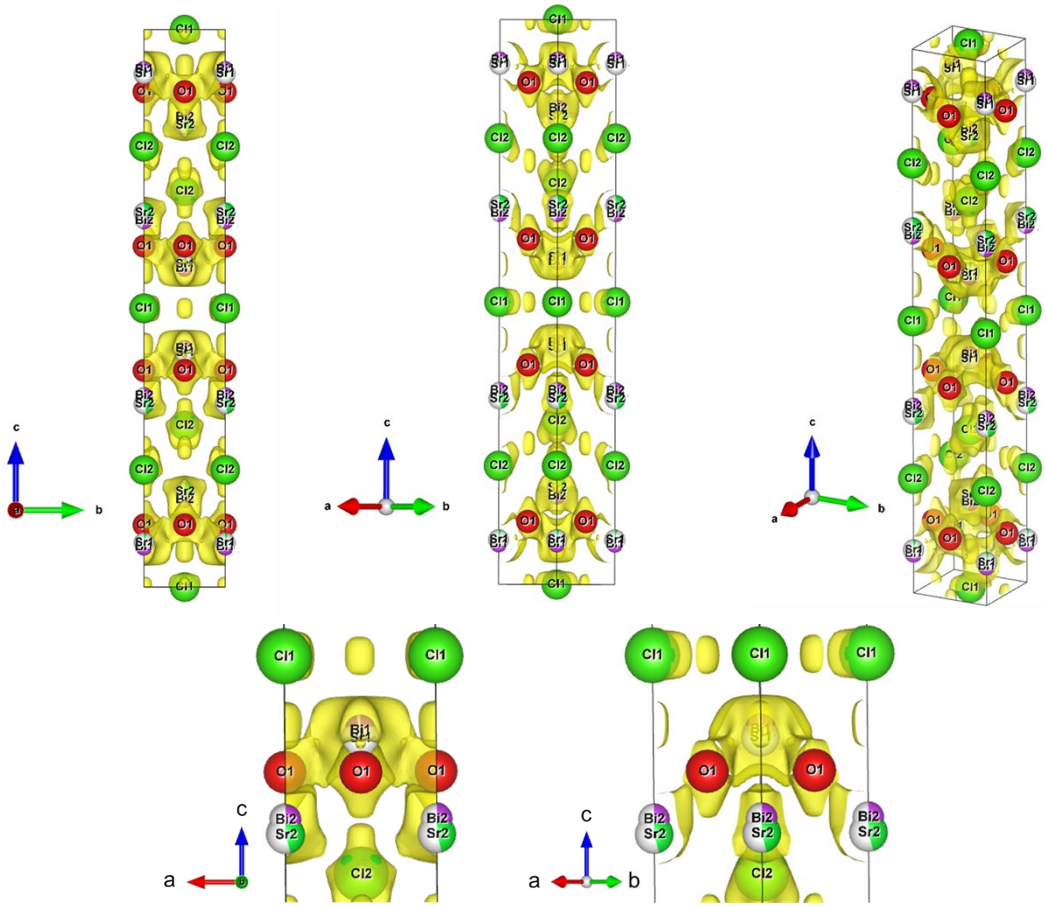

Figure S5 Electron density distribution of $SrBi_3O_4Cl_3$ obtained by MEM analysis (isosurface: 0.55 $Å^{-3}$).

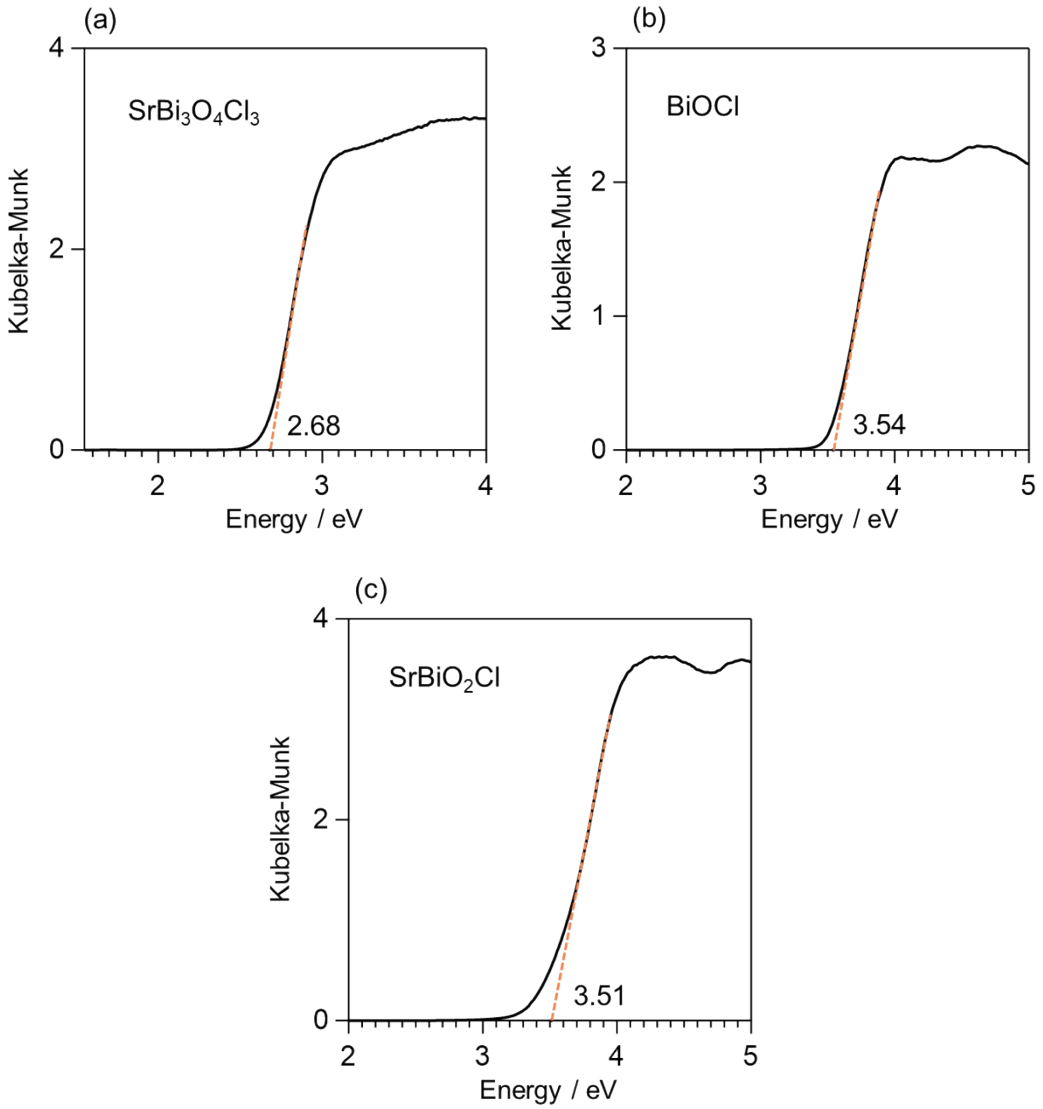

Figure S6 Determination of bandgaps of (a) $SrBi_3O_4Cl_3$, (b) BiOCl, and (c) $SrBiO_2Cl$

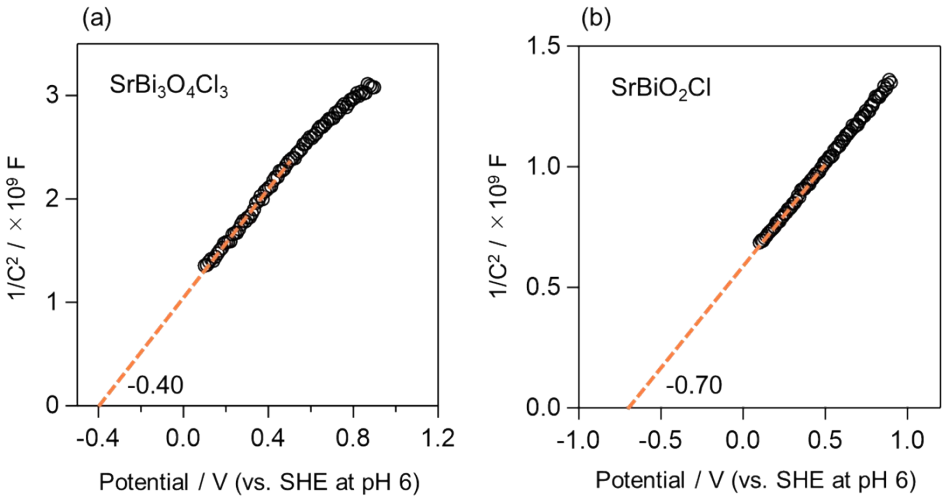

Figure S7 Mott-Schottky plots for (a) $SrBi_3O_4Cl_3$ and (b) $SrBiO_2Cl$.

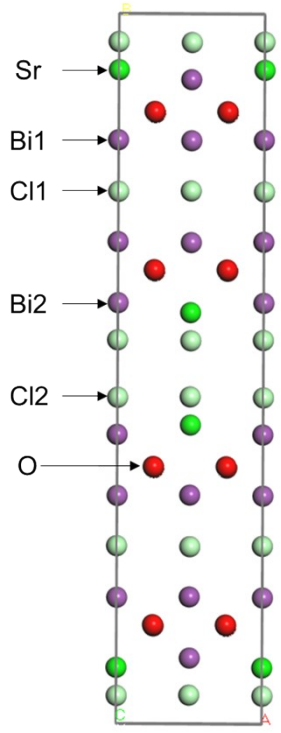

Figure S8 Structure of $SrBi_3O_4Cl_3$ with $\sqrt{2} \times \sqrt{2} \times 1$ supercell used for DFT calculation.

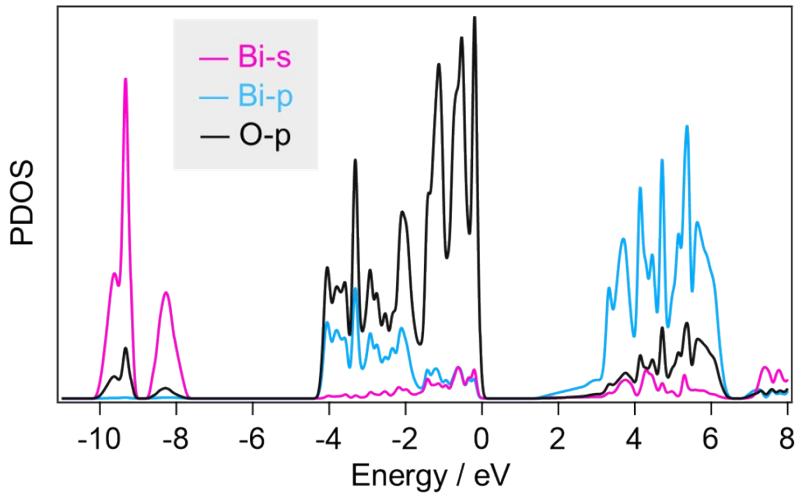

Figure S9 PDOS of $SrBi_3O_4Cl_3$ for 6s and 6p orbitals of Bi, along with that of O.

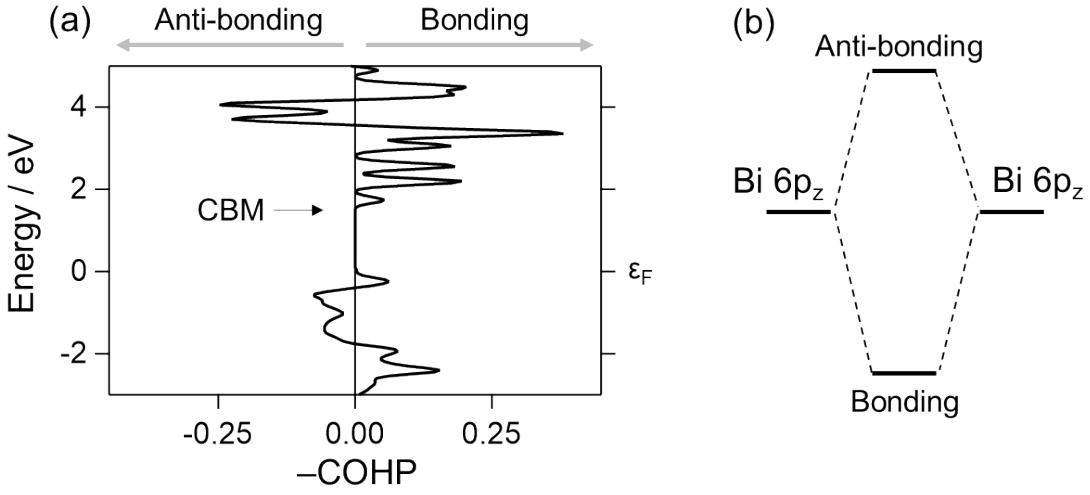

Figure S10 (a) COHP for the interaction of Bi 6pz–Bi 6pz. (b) Schematic image of the interaction.

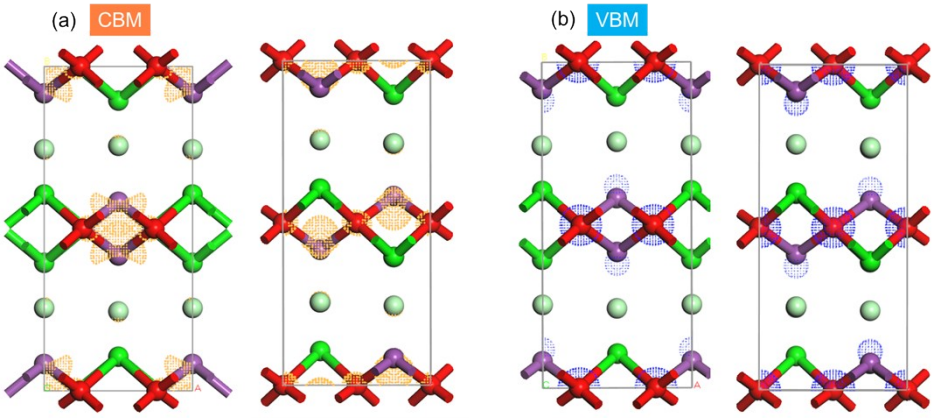

Figure S11 Orbital distributions of the CBM (orange) and VBM (blue) of $SrBiO_2Cl$ estimated by DFT calculations (Isosurface value: 0.02 e/Å^3), which are viewed from two different directions.

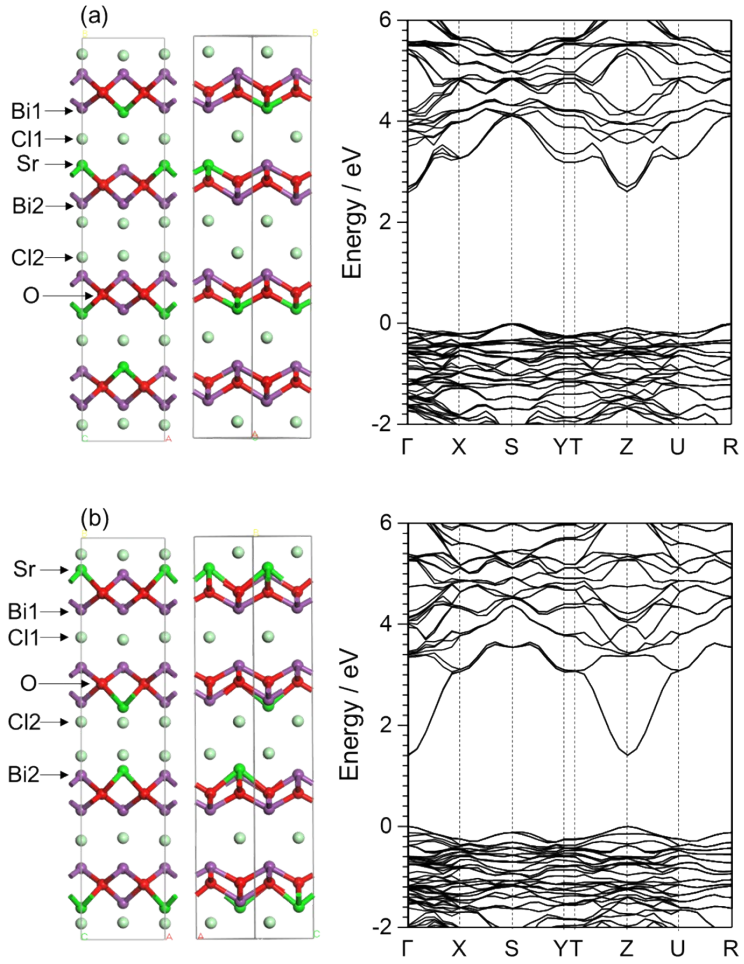

Figure S12 Band structure of the two models: (a) one with Bi/Sr1 site occupied by Bi^{3+} and Sr^{2+} (b) the other with Bi/Sr1 site fully occupied by Bi^{3+}.

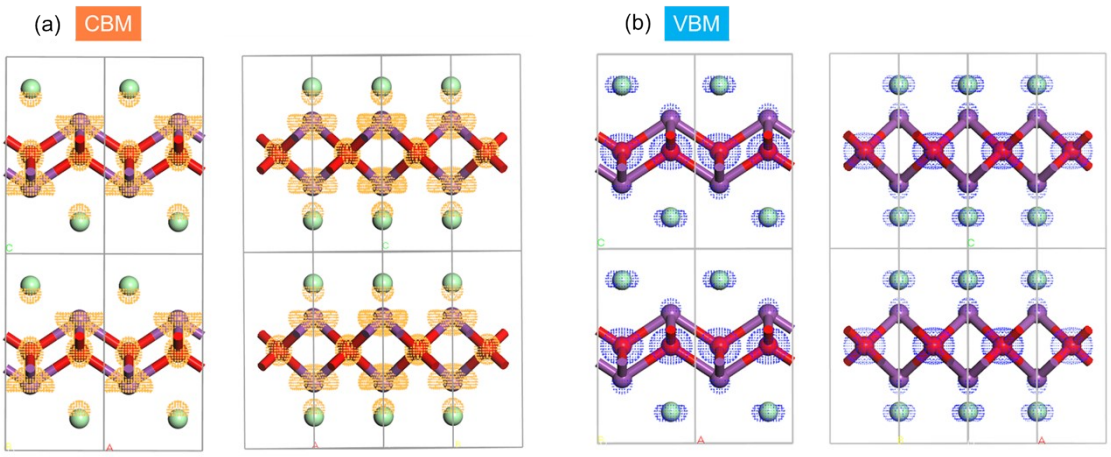

Figure S13 Orbital distributions of the CBM (orange) and VBM (blue) of BiOCl estimated by DFT calculations (Isosurface value: 0.06 e/Å^3), which are viewed from two different directions.

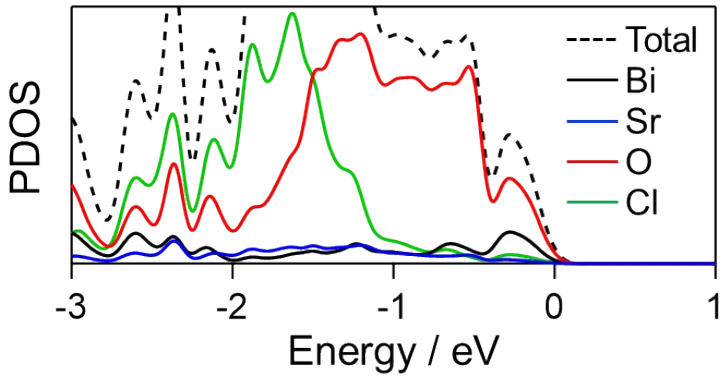

Figure S14 Valence band structure of $SrBiO_2Cl$ reproduced from the reference.[S1]

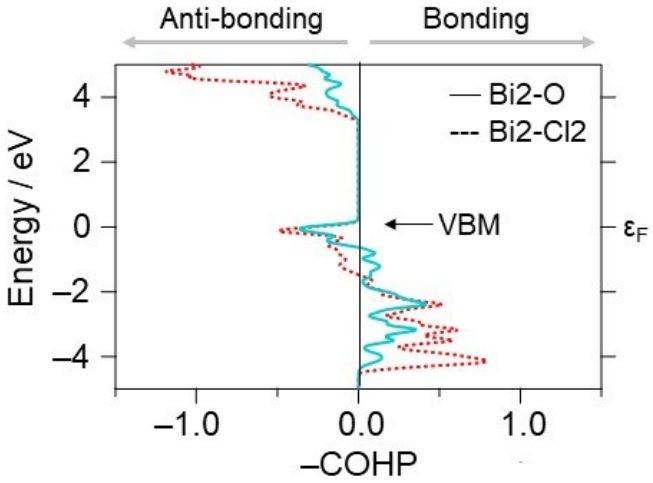

Figure S15 COHP for the interaction of Bi2–O and Bi2–Cl2.

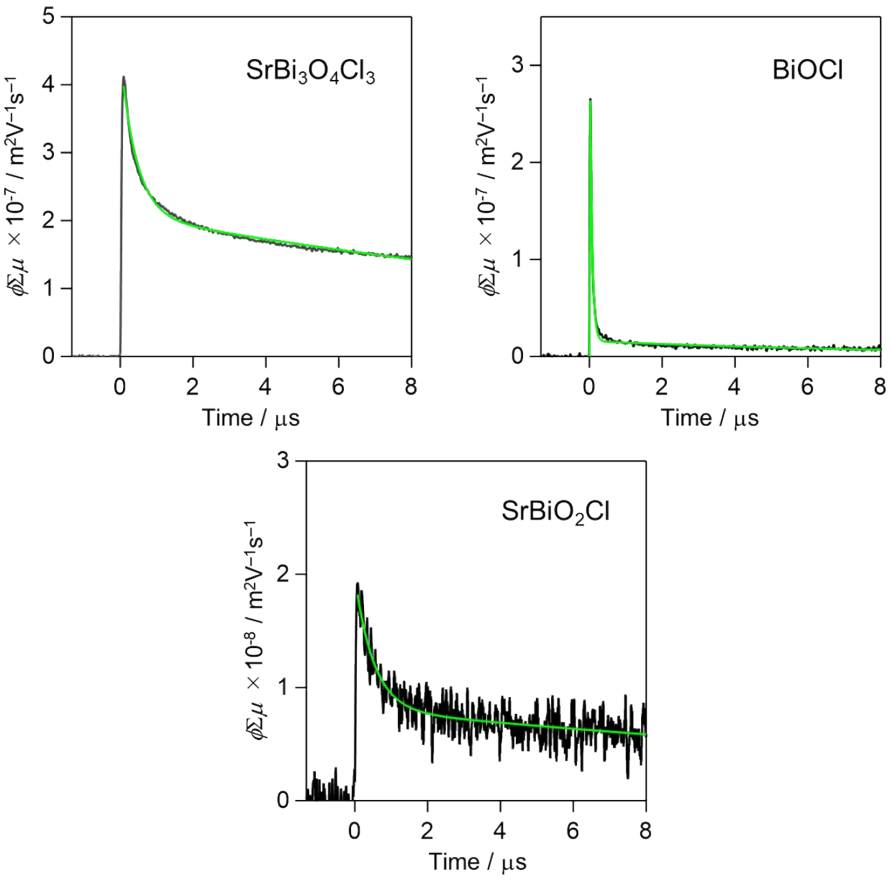

Figure S16 Fitting of the TRMC kinetics of $SrBi_3O_4Cl_3$, BiOCl, and $SrBiO_2Cl$ using biexponential function ($A_1\exp(-k_1t) + A_2\exp(-k_2t)$) (the solid green line).

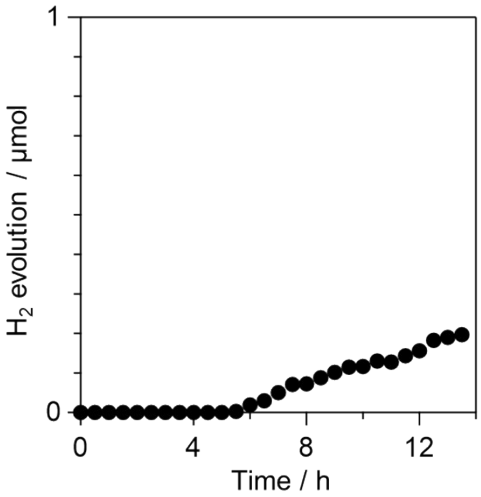

Figure S17 Time course of photocatalytic H_2 evolution on $SrBi_3O_4Cl_3$ (100 mg) with in situ photodeposition of a Pt cocatalyst (1 wt%) under UV-vis light ($300 < \lambda < 500$ nm) from an aqueous methanol solution (10 vol%, 120 mL).

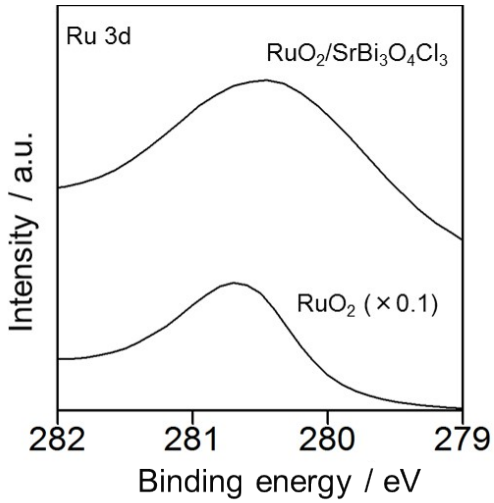

Figure S18 XPS spectrum of $RuO_2/SrBi_3O_4Cl_3$ in the Ru 3d region.

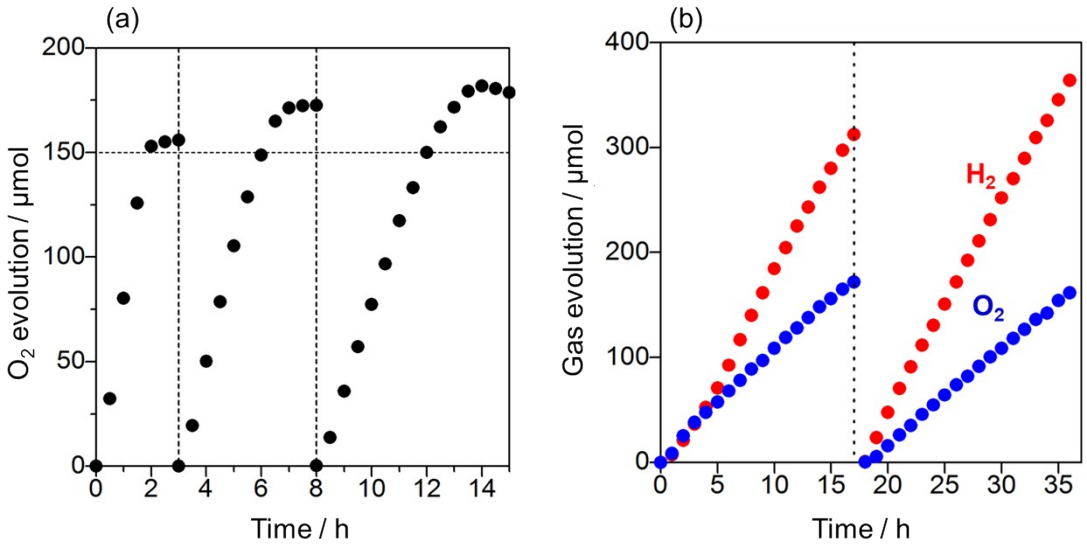

Figure S19 (a) Time courses of photocatalytic O_2 evolution on $RuO_2/SrBi_3O_4Cl_3$ (100 mg) under visible light ($400 < \lambda < 800$ nm) from an aqueous solution of $FeCl_3$ (5 mM as Fe^{3+}, 120 mL, pH 2.4 adjusted by HCl)**.** An excess of O_2 over the stoichiometric amount estimated from the amount of introduced Fe^{3+} (150 μmol) was observed in the case of $FeCl_3$. The decomposition of $SrBi_3O_4Cl_3$ and the formation of BiOCl may be related to the excess amount of O_2. (b) Z-scheme overall water splitting using $RuO_2/SrBi_3O_4Cl_3$ (50 mg) as O_2-evolving photocatalyst and $Ru/SrTiO_3$:Rh (50 mg) as H_2-evolving photocatalyst under visible light ($400 < \lambda < 800$ nm) in an aqueous $FeCl_3$ solution (2 mM as Fe^{3+}, 120 mL, pH 2.4).

Reference

S1 H. Suzuki, H. Kunioku, M. Higashi, O. Tomita, D. Kato, H. Kageyama and R. Abe, *Chem. Mater.*, 2018, **30**, 5862-5869.